

Oxygen effect in Magnetron Sputtered Aluminum doped Zinc oxide films.

Saad Rahmane¹, Mohamed Abdou Djouadi², Mohamed Salah Aida³ and Nicolas Barreau²

1-Laboratoire de Chimie Appliquée, Université de Biskra, BP 145 RP, 07000 Biskra, Algérie.

E-mail: rahmanesa@yahoo.fr

2-Institut des Matériaux Jean Rouxel IMN UMR 6502, Université de Nantes, 2 rue de La Houssinière BP 32229, 44322 Nantes Cedex France.

3-Laboratoire des Couches minces et Interfaces, Université Mentouri, 25000 Constantine, Algérie.

Abstract:

In this work, polycrystalline transparent conductive aluminum doped zinc oxide (ZnO:Al) films, have been successfully grown on glass and silicon substrates by rf magnetron sputtering technique at room temperature. The effect of oxygen content in plasma on the structural, optical and electrical properties of the films was systematically studied. The growth rate was found to decrease with the increase in O₂ content. The crystal structure of ZnO:Al films deposited on glass is hexagonal with C-axis preferential orientation, while for film deposited on silicon substrate, the preferred orientation of crystallite shifts from (002) to (100) direction with the increase in O₂ content. Intrinsic stress increases with an increase of oxygen content, and near stress-free film was obtained at 0 % O₂ content. Low resistivity ($\rho = 1.25 \times 10^{-3} \Omega\text{cm}$) associated to high transmittance ($T > 92\%$) in the visible regions, were obtained for ZnO:Al film deposited at room temperature without oxygen content in the deposition chamber. From the optical characterization, we deduced that the band gap shifts towards lower energy with an increase of oxygen content.

Keywords: magnetron sputtering, Al doped ZnO, O₂ content, properties.

1. Introduction:

II-VI compound semiconductor zinc oxide (ZnO) has attracted much attention because of its interesting properties and its unique combination of electrical, optical, piezoelectric and acoustical properties. ZnO thin films have found many applications namely solar cells, energy windows, varistors, gas sensors [1-3], short wavelength light emitting diodes [4] and transparent electrodes [5]. This is due to their important properties characterized by a high transparency, and conductivity, a good thermal stability against the hydrogen plasma, non toxic and easy fabrication [6].

The physical properties of ZnO films prepared by rf magnetron sputtering depend mainly on the sputtering parameters such as sputtering power, argon gas pressure, substrate temperature and the target-substrate distance. In this paper, thin films of ZnO:Al are prepared by magnetron sputtering system. The mutual dependence of structural, optical and electrical properties of the samples as function of oxygen gas content is investigated.

2. Experimental procedure:

ZnO:Al films were deposited in magnetron sputtering system using a ZnO target (diameter 7.5 cm) mixed with 2 wt.% Al₂O₃. Prior the deposition, the base pressure in the chamber was 5×10^{-7} mbar. The target-substrate spacing, the sputtering power, and argon gas pressure were kept constant at 2.6 cm, 200 W and 2×10^{-3} mBar respectively. All the films were deposited at room temperature on glass and monocrystalline silicon (100) substrates. In order to investigate the influence of oxygen content in plasma on the ZnO:Al properties, the oxygen gas content in the deposition was varied from 0 % to 40 %.

Film thickness and substrate curvatures were measured with a stylus profilometer DEKTAK 3030. As most commonly used, the stress in our films has been calculated by the bend-bending method, where the radius of the coated substrate curvature is determined and used to calculate the residual stress. The internal stress in the

deposited film is calculated from the change in the substrate curvature from $1/R_0$ for the uncoated substrate to $1/R_e$ after film deposition, with the following Stoney's formula [9]:

$$\sigma = [(E_s e_s^2) / (6(1-\nu_s)e)] [(1/R_e) - (1/R_0)]$$

where R_0 is the radius of curvature of the Si substrate, R_e is the curvature radius after film deposition, E_s and ν_s are, respectively, the Young's modulus and Poisson ratio of the substrate, e_s and e are the thickness of the substrate and the film, respectively. The crystal structure of the films was studied by x-ray diffraction technique using a Siemens D 5000 system with Cu K_α ($\lambda = 0.15406$ nm). The structural investigation was also performed using high-resolution Transmission Electron Microscopy (HRTEM), a HF2000-FEG having 0.23 nm resolution and Jeol 6400 Scanning Electron Microscope (SEM). EDS (Energy Dispersive Spectroscopy associated to Jeol 5400 SEM) was used to determine the chemical composition of the films. A CARRY UV-Vis-NIR scanning spectrophotometer was used to record the optical transmittance.

The dc electrical resistivity measurement is achieved at room temperature with four-point probe, with the appropriate correction factors.

3. Results and discussions

ZnO:Al films deposited on glass and silicon substrates, were physically stable and had a good adherence to the substrates. The deposition rate was estimated from the film thickness and the corresponding time. The higher oxygen content resulted in lower growth rate of ZnO:Al films, as shown in figure 1. With a fixed total gas pressure, an increase in oxygen content in the gas chamber reduces the number of incident argon ions; the later are responsible for the target sputtering. Therefore, the growth rate decreases with increasing oxygen content. A high rates (114 nm/min on silicon and 106 nm/min on glass) are obtained at 0 % oxygen concentration, in some cases, this value is higher than the existing bibliographical references [10,11].

In EDS typical spectra shown in figure 2, peaks were appeared at 518, 1109 and 1496 eV, they are assigned to O- K_α , Zn- L_α and Al- K_α respectively. The estimated concentration of zinc, oxygen and aluminium was 50.5 at.%; 47.5 at.% and 2at.%, respectively. A clear variation of the concentration of the elements upon the oxygen content in plasma was not found. Due to the limitations of EDS technique, it must be considered that these results giving only an idea of the composition of the films.

XRD patterns of the ZnO:Al films deposited at different oxygen concentration on glass substrates are shown in figure 3(a). For all films, only the (002) diffraction peak at about 34° appears in the spectra, which indicates the ZnO:Al films are of hexagonal wurtzite crystal structure and that film growth is achieved along the C axis perpendicular to the substrate surface. It is noted that no diffraction peak from other phase is detected. At 0 % oxygen content, the diffraction intensity of the (002) direction is very high and the FWHM corresponding is 0.21° . With a further increase of the oxygen content, the diffraction intensity of the (002) direction decreases and the FWHM increased as can be seen in figure 4. The highest intensity and the smallest FWHM value of 0.21° for the film deposited at 0 % oxygen content, indicate that the crystallinity of the resulting films is improved when prepared with low O₂ content. This behaviour can be understood, by the decrease in the kinetic energy of the reactive particles in the plasma when oxygen concentration in the chamber is increased, which limits the surface diffusion of the growing atoms. This yields to the decrease in the films thickness and thus degrades the films quality.

By considering the (002) peak position in the standard data as reference position, we found that the peak position shifts towards lower angle value, this indicates the clear evidence of the existence of compressive stress in the film network, especially in the films deposited at high oxygen content. Figure 4 shows the stress versus the oxygen content, the stress is compressive and varies from 1.1 (GPa) to nearly free of stress when the oxygen concentration decreases from 40 % to 0 %. This is attributed to the improvement in crystallinity. A similar value of stress was reported in the literature [12, 13]. The increase in the film stress with increasing oxygen can be due to the fact that, the oxygen atoms in excess will occupy interstitial sites which cause network distortion.

Figure 3(b) displays XRD patterns of ZnO:Al films deposited on silicon substrate at different O₂ concentration. It can be seen that with the increase in oxygen content, the intensity of (100) plane increases. However, the intensity of (002) plane shows a decreasing trend and disappears completely for high O₂ content. Furthermore, with increasing oxygen content, the FWHM of (100) plane becomes narrower which indicates an improvement in the structural order of ZnO:Al films. The most attractive feature is that by increasing the oxygen concentration, the preferred orientation of crystallite shifts from (002) to (100) directions. However, as reported above, in the case of glass substrate the growth plane remains preferentially (002). This discrepancy in

the preferential orientation with the nature of the used substrate may originate from the growth process involved during film growth, especially at the earlier stage of growth, i.e the nucleation step. Further study is necessary to elucidate this difference. Regardless the deposition technique, it is generally reported that ZnO thin films grow with the (002) direction [14-17] which correspond to the growth along the direction c normal to the substrate surface. This preferential orientation is believed to be due to the low energy of this plane [18]. With increasing the deposition temperature or film doping, the preferential growth direction disappear and other plane emerge in the diffraction pattern, namely (100) and (101) [19-21].

The influence of the deposition condition on the occurrence or not of a privileged direction can be linked to the films growth mechanism and the role played by the deposition conditions.

Despite the numerous works on ZnO thin films there are no much publications describing the growth mechanism. Indeed, the deposition mechanism of ZnO thin films passes through the nucleation and the subsequent growth. The growth direction is governed by the «survival of the fastest» as proposed by Drift [22]. The nucleation with various orientations can be formed at the initial stage of the deposition and each nucleus competes to grown. It was reported in sputtered ZnO that at high deposition rate the less density packed atomic planes are preferentially oriented [23]. The less densely packed orientation (100) ($5.91 \cdot 10^{14}$ atm/cm²) rather than the plane (002) ($10.93 \cdot 10^{14}$ atm/cm²), this can be explain the shift of the preferred orientation of crystallite from (002) to (100) directions.

The films surfaces were analysed by SEM, figure 5 presents a typical surface and cross-sectional SEM image of the film deposited with oxygen content 0 %. The film displays a granular surface, uniform grain size and void free. From the cross-sectional image, it is seen that the film is composed with columnar structures, which is consistent with the highly (002) texture growth evidenced by XRD analysis. The columnar morphology of our films is confirmed by the micrograph of TEM shown in figure 6.

In figure 7 we have reported the optical transmittance spectra for ZnO:Al films deposited at various oxygen content, the fluctuation in the spectra is principally due to the interface effect owing the reflexion at interfaces. Sharp fundamental absorption edges are observed in all the spectra corresponding to the ZnO:Al films. These films have a high transmittance (>92%) in visible regions and high absorption (near 100%) in ultraviolet regions. As the oxygen content is above to 0 %, the average transmittance of the films reduces slightly. It would be noted that the film deposited at 0 % oxygen content becomes nearly opaque to near infrared region. This is due to the highest carrier concentration, which absorb photons [24]. Figure 8 shows the variation of band gap and Urbach tail as a function of oxygen concentration. The blue shift of the absorption edge with decreasing oxygen content is mainly attributed to the Burstein-Moss effect [25,26], since the absorption edge of degenerate semiconductor is shifted to shorter wavelength with increasing carrier concentration [27]. This decrease in the band gap energy with increasing oxygen content is confirmed by the decrease in band tail width. The variations of E_g and E_U can be explained by the decrease in growth rate with the increase in oxygen concentration. The value of E_U obtained for undoped ZnO prepared by sol-gel [28] and CVD techniques [29] is reported to be in the range of 0.07 – 0.10 eV. The larger values of E_U (0.15 – 0.18 eV) obtained in the present study indicates the presence of a large concentration of localised donor states in the band gap.

Low films resistivity ($\sim 1.25 \cdot 10^{-3}$ Ωcm) can be achieved without oxygen in the deposition chamber. Also the resistivity increases significantly with increase in oxygen content. This variation of resistivity is ascribed to the change in carrier concentration and/or mobility which are the characteristic parameters reflecting the films structure. It can be seen that at the position of the stress minimum corresponds the minimum in the measured resistivity. This indicates the clear evidence of the correlation between intrinsic stress and electrical parameters of ZnO:Al films. Low mechanical stress, i.e., a low concentration of crystallographic defects leads to better electrical properties.

4. Conclusion:

In summary, highly transparent and lower resistive ZnO:Al films were deposited at room temperature on silicon and glass substrates using rf magnetron sputtering technique. A systematic study was made on the influence of oxygen content in plasma, on the structural, optical and electrical properties of our films.

X-ray diffraction studies indicated that the films deposited on glass were polycrystalline in nature with (002) orientation axis perpendicular to the substrate surface. The FWHM of the films decreased to 21° with increasing oxygen content. For ZnO:Al films deposited on silicon we have found that by increasing the oxygen

concentration, the preferred orientation of crystallite shifts from (002) to (100) directions, this could be due to the nucleation process during film formation.

The film stress is compressive, it decreases from 1.1 (GPa) to nearly stress free with reducing oxygen content in the deposition chamber. The decrease in the intrinsic stress is probably the reason for the observed improvement of film crystallinity.

All films have a high transmission greater than 90% in visible region > However, the film deposited without oxygen in the deposition chamber is nearly opaque in near infrared region. This is due to photons absorption by the large concentration of free electron present in film network; this is consistent with the low measured electrical resistivity ($\sim 1.25 \times 10^{-3} \Omega\text{cm}$) in film deposited without adding oxygen in the chamber. The optical band gap shifts towards lower energy with an increase of oxygen content.

References

- [1] Chopra K L, Major S and Pandya D K 1983 *Thin Solid Films* **102** 1.
- [2] Aranovich J J, Golmaza D, Fohrenbruck A L and Bube R H 1980 *J. Appl. Phys.* **51** 4260.
- [3] Olvera M L, Maldonado A, Asomoza R, Komagai M and Azomosa M 1993 *Thin Solid Films* **229** 196.
- [4] Tang Z K, Wong G K L, Yu P, Kawasaki M, Ohtomo A, Koinuma H and Y. Segawa 1998 *Vacuum* **72** (25) 3270.
- [5] Hoffman R L, Norris B J and Wagera J F 2003 *Appl. Phys. Lett.* **82** 733.
- [6] Jin Z C, Hamberg J and Grangvist C G 1988 *J. Appl. Phys.* **64** 5117.
- [7] Abdallah B, Chala A, Jouan P-Y, Besland M P and Djouadi M A 2007 *Thin Solid Films* **515** 7106.
- [8] Jeong S H and Boo J H 2004 *Thin Solid Films* **447-448** 105.
- [9] Lee J, Lee D, Lim D and Yang K 2007 *Thin Solid Films* **515** 6094.
- [10] S. Rahmane, M.A. Djouadi, M.S. Aida, N. Barreau, B. Abdallah, N. Hadj Zoubir, *Thin Solid Films* 519 (2010) 5–10.
- [11] Hinze J and Ellmer K 2000 *J. Appl. Phys.* **88** 2443.
- [12] Lokhand B J, Patil P S and Uplane M D 2000 *Mater.Lett.* **57** 573.
- [13] Mass J, Bhattacharya P and Katiyar R S 2003 *Mater.Sci. and Eng. B* **103** 9.
- [14] Ondo-Ndong R, Pascal-Delannoy F, Boyer A, Giani A and Foucaran A 2003 *Mater.Sci. Eng.B* **97** 68.
- [15] Nakanishi Y, Miyake A, Kominami H, aoki T, Hatanaka Y and Shimaoka G 1999 *Appl.Surf.Sci.* **142** 233.
- [16] Shu Y, Water W and Liaw J T 2003 *J.Eur.Ceram.Soc.* **23** 1593.
- [17] Zhang C, Li X, Bian J, Wu W and Gao X 2004 *Sol.Stat.Commun.* **132** 75.
- [18] Nunes P, Fortunato F and Martins R 2001 *Thin Solid Films* **383** 277.
- [19] Goyal D J, Agshe C, Takwale M G, Bhide V G, Mahamuni S and Kulkarni S K 1993 *J.Mater.Res.* **8** 1052.
- [20] Van der Drift A 1967 *Philips Res.Rep.* **22** 267.
- [21] Murti D K and Bluhm T L 1982 *Thin Solid Films* **87** 57.
- [22] Timothy J. Coutts, David L.Young, and Xiaonan Li 2000 *MRS BULLETIN* 58.
- [23] Burstein E 1954 *Phys. Rev.* **93** 632.
- [24] Moss T S 1954 *Proceedings of the physical Society London* **B76** 775.
- [25] Lee G H, Yamamoto Y, Kouroggi M and al. 2001 *Thin Solid Films* **386** 117.
- [26] Natsume Y, Sakata H 2000 *Thin Solid Films* **372** 30.
- [27] Natsume Y, Sakata H and Hirayama T 1995 *Phys. Stat. Solid. (a)* **148** 485.

Figures Caption

Figure 1: Variation of deposition rate versus oxygen content.

Figure 2: EDS spectrum for ZnO:Al film deposited at 10 % O₂ content.

Figure 3: X- ray diffraction patterns of ZnO:Al films prepared at different oxygen content (a) on glass and (b) on silicon.

Figure 4: Variation of FWHM and intrinsic stress with oxygen content in the deposition chamber.

Figure 5: SEM images showing the (a) cross-sectional and (b) surface of ZnO:Al film grown at 10 % oxygen content.

Figure 6: TEM Micrograph of ZnO:Al film.

Figure 7: Optical transmittance of ZnO:Al films deposited at various oxygen composition in the deposition gas.

Figure 8: Variation of band gap and band tail width on oxygen content in the deposition chamber.

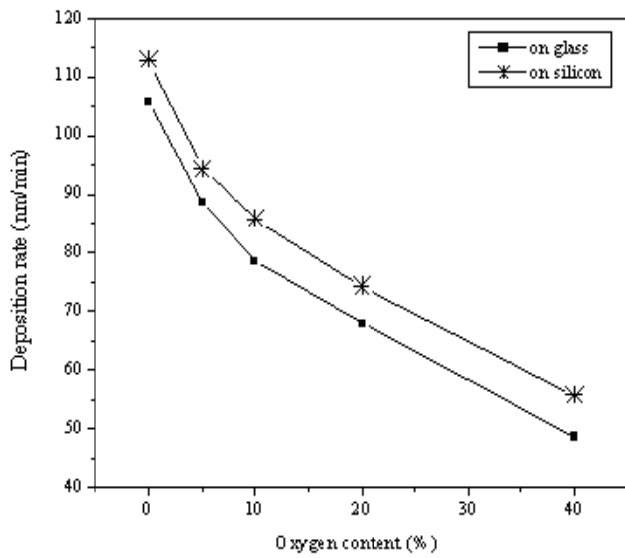


Figure 1

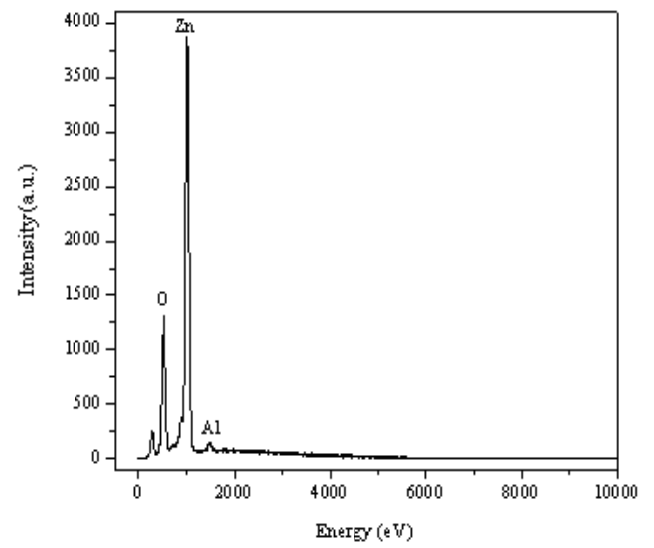


Figure 2

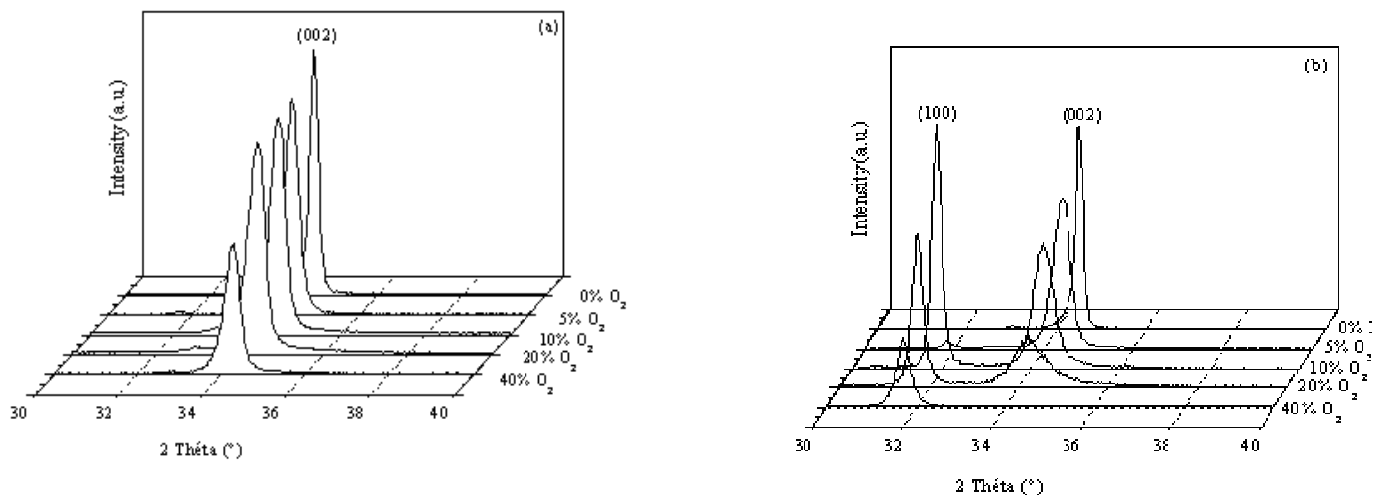


Figure 3

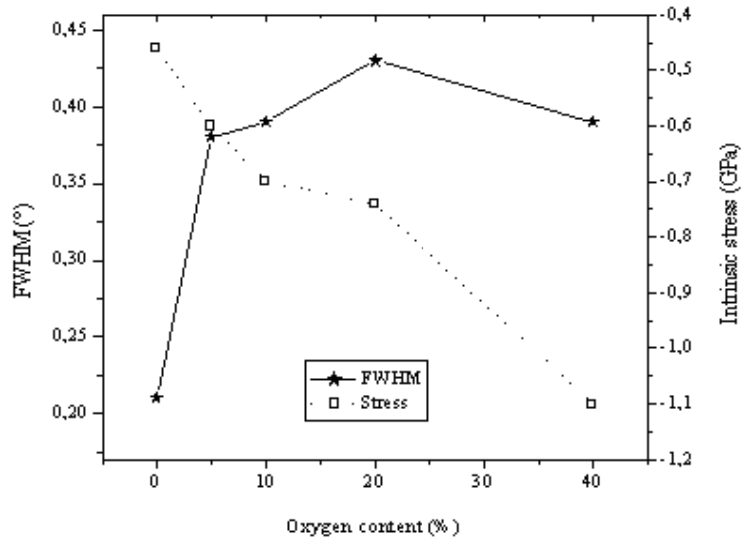


Figure 4

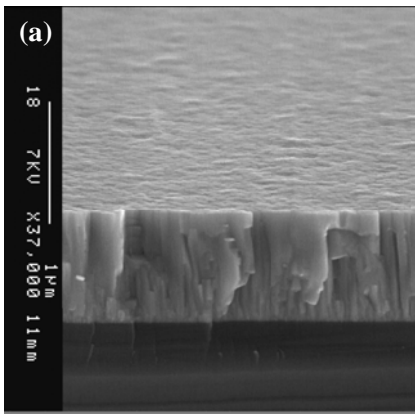


Figure 5

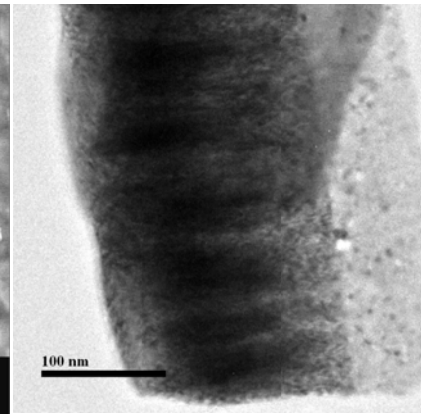
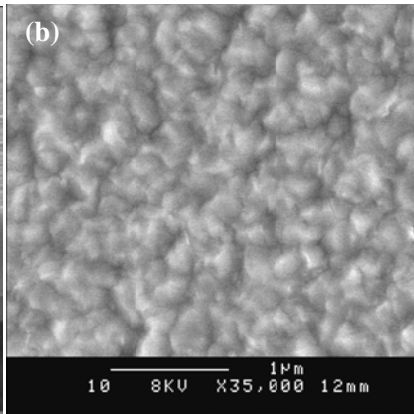


Figure 6

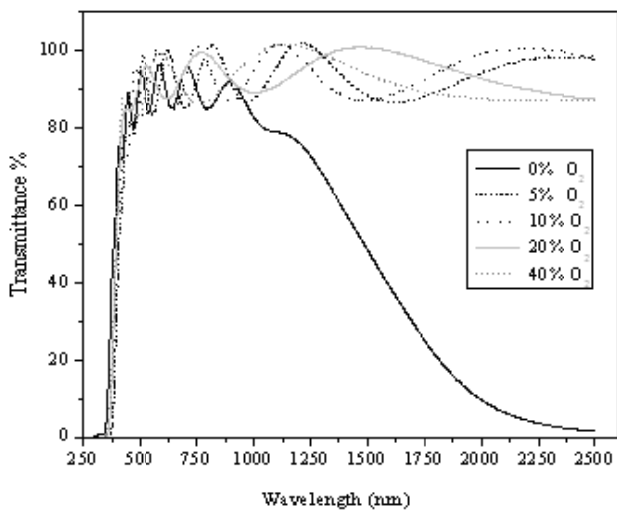


Figure 7

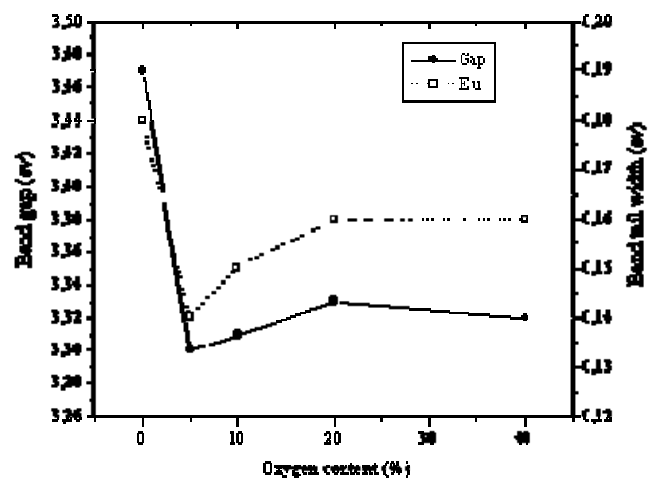


Figure 8